Danish Meteorological Institute
Ministry for Climate and Energy

Danish Climate Centre Report 09-09

Inferring magnetic crustal thickness and geothermal heat flux from crustal magnetic field models

Cathrine Fox Maule, Michael E. Purucker and Nils Olsen

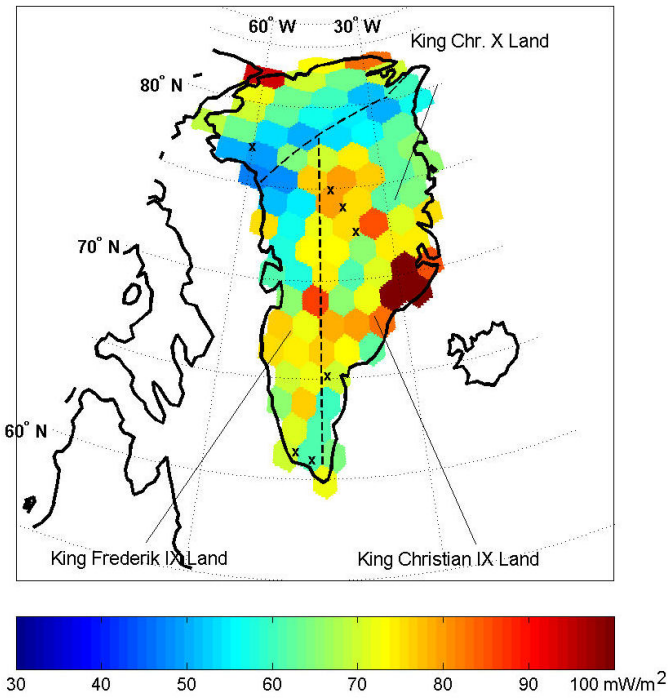

Colophone

Serial title:
Danish Climate Centre Report 09-09

Title:
Inferring magnetic crustal thickness and geothermal heat flux from crustal magnetic field models

Subtitle:
Estimating the geothermal heat flux beneath the Greenland ice sheet

Authors:
Cathrine Fox Maule, Michael E. Purucker and Nils Olsen

Other Contributers:
-

Responsible Institution:
Danish Meteorological Institute

Language:
English

Keywords:
Heat flow, geomagnetism, Greenland, Australia

Url:
www.dmi.dk/dmi/dkc09-09

ISSN:
1399-1957

ISBN:
978-87-7478-585-9 (online)

Version:
1

Website:
www.dmi.dk

Contents

Colophone . . . 2
1 Abstract **4**
2 Introduction **5**
3 Modelling the magnetic crustal thickness **6**
3.1 Results for the magnetic crustal thickness . . . 11
3.1.1 Australia . . . 13
3.1.2 Greenland . . . 15
3.1.3 Difference between 3SMAC and CRUST2.0 . . . 16
4 Thermal model of the crust **16**
4.1 Results for the geothermal heat flux . . . 20
4.1.1 Australia . . . 20
4.1.2 Greenland . . . 21
5 Discussion of errors **24**
6 Concluding remarks **26**

1. Abstract

High quality magnetic measurements from recent satellites like Ørsted and CHAMP have greatly improved the spatial resolution of crustal magnetic field models, which opens new possibilities for geophysical and geological interpretation. Here, we present the results of a method using magnetic field models to determine the thickness of the magnetic crust, from which estimates of the geothermal heat flux are attempted. The thickness of the magnetic crust is determined globally from a crustal field model by the equivalent source magnetic dipole method. We find that the magnetic crustal thickness of the continental crust is typically between 20 and 50 km; in local areas it may exceed 60 km or be less than 20 km. Comparison of our results of the magnetic crustal thickness with independent results by others indicates that our method correctly reflects thermal conditions at depth.

To estimate the geothermal heat flux, a thermal model of the crust is derived, based on the assumption that the lower boundary of the magnetic crust coincides with the Curie isotherm. We apply a 4-layer model for the thermal conductivity and the heat production of the crust, using different values and expressions for their variation in the sediment, upper, middle, and lower crustal layers. For the estimates of the heat flux we have chosen to focus on two specific areas, Australia and Greenland. The first area is interesting as other independent data are available for evaluating whether the model produces reasonable results. The second area is of interest as direct heat flux measurements, and in particular a nationwide map of the spatially varying heat flux, is difficult to obtain and important for applications such as ice sheet modelling. With the proposed method we estimate the spatially varying heat flux with a resolution of a few hundred kilometres.

2. Introduction

The high quality magnetic field data that have been obtained by the Ørsted, CHAMP and SAC-C satellites have led to an increased understanding of the Earth's magnetic field. During these missions new magnetic field models of increased complexity and resolution have continuously been developed (e.g. Olsen *et al.*, 2000; Olsen, 2002; Sabaka *et al.*, 2004; Olsen *et al.*, 2006; Maus *et al.*, 2007). The new data have, amongst other things, led to a more detailed description of the crustal field, which encourages geophysical and geological interpretations (Hemant & Maus, 2005; Maus *et al.*, 2007). To investigate one potential application of field models, we have developed a method to estimate the magnetic crustal thickness and from this attempt to estimate the geothermal heat flux. We have chosen to focus on that quantity for two reasons. First, many studies (e.g. Hamoudi *et al.*, 1998; Tanaka *et al.*, 1999) have observed a correlation between magnetic data (both aeromagnetic and satellite data) and the geothermal heat flux, which indicates that it may be feasible to determine the heat flux from magnetic data. Secondly, such a method can be used to estimate the spatial variability of the geothermal heat flux underneath the polar ice caps (Fox Maule *et al.*, 2005). Little is currently known about how the heat flux varies underneath the ice. Direct heat flux measurements are difficult and expensive to obtain, so information about the heat flux variation currently rely on indirect methods of obtaining heat flux estimates. The heat flux influences the basal conditions of the ice sheets (Greve, 2005), and therefore maps of spatially varying heat flux is an important boundary condition in ice sheet modelling, which for example are used to predict the response of ice sheets to climate change.

Magnetic data can reveal information about the thermal state of the crust as the magnetic properties of crustal rocks depend on temperature. Rocks below their Curie temperature may sustain induced or remanent magnetization, but rocks heated above their Curie temperature become practically non-magnetic. The magnetic mineral believed to be responsible for most of the crustal magnetization is magnetite (e.g. Schlinger, 1985; Frost & Shive, 1986; Clark & Emerson, 1991). Magnetite, which can be strongly magnetized, is a minor but ubiquitous mineral in the crust and has a Curie temperature of about 580°C.

From magnetic data it is possible to estimate the depth of the Curie isotherm, called the Curie depth. Aeromagnetic data have been widely used for this purpose (e.g. Okubo *et al.*, 1985; Tsokas *et al.*, 1998; Tanaka *et al.*, 1999; Stampolidis & Tsokas, 2002), and it has in many of these studies been noticed that the obtained depths correlate well with the heat flux: high heat flux is found in areas of shallow Curie depth and vice versa. Magnetization models of the crust derived from satellite magnetic data have also demonstrated a correlation between Curie depth estimates and surface heat flux (e.g. Mayhew, 1982a,b, 1985; Hayling, 1991; Mayhew *et al.*, 1991; Purucker *et al.*, 1998; Hamoudi *et al.*, 1998); these previous models were however, based on data from the earlier POGO and Magsat satellites. Our study differs from the previous ones in that it is based on high quality satellite data from the current missions. Additionally, we suggest that the Curie depths estimated from the magnetic crustal thickness obtained from magnetic data can be used to estimate the heat flux in areas where direct heat flux measurements cannot readily be made. In a previous paper, Fox Maule *et al.* (2005), we presented an application of our method to infer heat flux in Antarctica; the present paper presents global results for the magnetic crustal thickness based on a more recent crustal field model as well as results for the heat flux in Australia and Greenland. The estimation of the magnetic crustal thickness have been improved by including the north-south

component of the magnetic field besides the radial component in its determination as opposed to only using the radial component previously. The thermal model has been improved by dividing the igneous crust into several layers (upper, middle and lower crust) with different thermal parameters and by including a sediment layer.

Using a field model instead of the raw satellite magnetic field observations is necessary as the magnetic field measured by a satellite contains contributions from several different sources: the core, the crust, the ionosphere and the magnetosphere. Only the field from one of these sources, the crust, is related to the heat flux. Field modelling allows (to some extent) for a separation of the various sources (e.g. Sabaka *et al.*, 2004), and the crustal field can thereby be isolated. Some field models such as MF5 by Maus *et al.* (2007) are designed especially to describe the high-degree crustal field.

Two issues are addressed in this study. The first, which concentrates on the magnetic properties of the crust, is to determine the thickness of the magnetic crust from which the depth to the Curie isotherm in continental regions is estimated; this is described in Section 3 and the results are presented in Section 3.1. The second issue, which focuses on the thermal properties of the crust, concerns thermal modelling of the crust based on knowledge of the depth of the Curie isotherm, from which an estimate of the heat flux is made; this is described in Section 4 and results are presented and discussed in Section 4.1. An assessment of the errors is given in Section 5.

3. Modelling the magnetic crustal thickness

The magnetic crust is that part of the crust which can sustain remanent or induced magnetization. It is bounded by the bedrock surface above and by the Curie isotherm or possibly Moho below. It is still unknown whether mantle rocks can be more than weakly magnetized over large scale areas (Wasilewski & Mayhew, 1992; Blakely *et al.*, 2005) and thus whether the magnetic crust may extend below Moho. The most likely region for large scale mantle magnetizations (Blakely *et al.*, 2005) may be in the vicinity of subduction zones. However, in regions where the Curie isotherm is at shallower depth than Moho, it will constitute the lower boundary of the magnetic crust, which is likely to be the case in widespread continental areas, where the crust is thick.

To determine the thickness of the magnetic crust we use a combined CHAOS/MF5 field model. The MF5 crustal field model of Maus *et al.* (2007) is a spherical harmonic (SH) expansion from degree 16 to degree 100 based on CHAMP data, with coefficients above degree 80 damped. However, the CHAOS model of Olsen *et al.* (2006) gives arguably a better description of the low-degree crustal field (see Olsen *et al.*, 2006) than the MF-series of crustal field models (e.g. Maus *et al.*, 2006, 2007), which are based on high-pass filtered data. Therefore we use the coefficients of the CHAOS model for degrees 16 to 40 and the coefficients of MF5 for degrees 41 to 100; the maximum degree of 100 corresponds to a horizontal wave-length of about 420 km at CHAMP altitude (200 km half wave-length resolution at surface level). We discretize the problem and use the combined CHAOS/MF5 field model to calculate the crustal field at a number of points, which we call observation points. For the geographical distribution of the observation points we use a spherical icosahedron grid (Covington, 1993) with 21,162 grid points (corresponding to a mean distance of 163 km between the observation points); this grid has the advantage of being of equal area securing an even weighting of the data. As altitude we choose 300 km, which is immediately below the lowest CHAMP observations.

Since the CHAOS/MF5 field model contains only SH coefficients above degree 15, the model does not account for the long wavelength part of the crustal field; i.e. it does not include the continent-ocean length-scale variation (Holme & Olsen, 2002). Separating the core and crustal field, in particular at intermediate SH degrees (14–16) where the fields are of roughly the same magnitude, is a classical problem in geomagnetism. Currently, no better technique of separating the core and crustal field than simple bandpass filtering exists. This will result in losing information about some long-wavelength structure of the crustal field and retaining some unwanted short-wavelength part of the core field. Applied to our problem of solving for the magnetic crustal thickness this means that the long-wavelength variation of the magnetic crustal thickness has to be obtained by other means, as will be discussed later.

Both induced and remanent magnetization of the crustal rocks contribute to the crustal field. The induced magnetization depends on the thickness of the magnetic crust, which is the parameter relevant for determining the heat flux, as well as on the strength of the inducing field and the susceptibility of the rocks. Only the induced part of the crustal field is relevant for estimating the magnetic crustal thickness and the heat flux. It is not possible to measure the induced part directly; however, a model of the remanent magnetization of the oceanic crust based on ocean floor ages, polar wander, and plate motion has been constructed by Dyment & Arkani-Hamed (1998b) and later improved by Purucker & Dyment (2000). Such a model of the remanent magnetization allows for isolation of the induced field by simply subtracting the remanent field from the observed field. However, the model of the remanent field includes only the oceanic and not the continental lithosphere. Unfortunately, no corresponding model of the remanent magnetization of the continental crust exists, most likely because it behaves much less systematically than the oceanic crust. However, a recent study indicates that induced magnetization is capable of explaining most of the continental crustal anomalies (Hemant & Maus, 2005), thus we neglect remanent magnetization in the continental crust and assume that the observed continental magnetization is purely induced. To obtain the observed induced field we therefore subtract the remanent magnetization model of oceanic crust by Dyment & Arkani-Hamed (1998b) and Purucker & Dyment (2000) from the observed field given by the CHAOS/MF5 model.

We use the equivalent source magnetic dipole (ESMD) method to estimate the magnetic crustal thickness from the observed induced field. In this method, which is described in some detail in Dyment & Arkani-Hamed (1998a) and Chapter 5 of Langel & Hinze (1998), the crustal magnetization is represented by a large number of dipoles distributed over the area of interest. The magnetic moments of the dipoles are then determined such that their combined magnetic field resembles the observed field at some given altitude, in our case 300 km. Using the standard spherical geographical coordinate system, the magnetic field is derived as the negative gradient of a scalar magnetic potential V, which, at observation point $\mathbf{r}_i = (r_i, \theta_i, \phi_i)$, is produced by J dipoles located at $\mathbf{r}_j$ for $j = 1,2 \ldots, J$:

$$V(\mathbf{r}_i) = \frac{\mu_0}{4\pi} \sum_{j=1}^{J} \mathbf{m}_j \cdot \nabla_j \left(\frac{1}{r_{ij}} \right), \tag{3.1}$$

where $\mu_0 = 4\pi{\cdot}10^{-7}$ Vs/Am is the vacuum permeability, $\mathbf{m}_j$ is the dipole moment of the jth dipole, ∇_j is the spherical gradient operator acting on the j-coordinates, and r_{ij} is the length of the vector

$$\mathbf{r}_{ij} = \mathbf{r}_i - \mathbf{r}_j. \tag{3.2}$$

To avoid edge effects we apply the ESMD method globally and represent the magnetization of Earth's crust by 21,162 dipoles distributed on the same icosahedral grid as the observation

points, but at Earth's surface. The inter-dipole distance of the crustal dipoles should be less than the half wave-length of the field model in order to resolve it. The inter-dipole distance constrains the altitude used for the observation points; to avoid overfitting of noise, the altitude must be large enough that the dipole discretization cannot be discerned.

The moment of each dipole is related to the average crustal magnetization, $\mathbf{M}_j$, of the volume represented by the dipole as

$$\mathbf{m}_j\left(\mathbf{r}_j\right) = \mathbf{M}_j\left(\mathbf{r}_j\right) h_j \; w_j, \tag{3.3}$$

where h_j is the thickness and w_j the surface area of the jth crustal block. Thus, the dipole moment of each crustal block depends on the thickness of the magnetic crust at the given place.

The induced magnetization, $\mathbf{M}$, of the crust is related to the inducing field, $\mathbf{B}$, by

$$\mathbf{M}\left(\mathbf{r}\right) = \frac{\kappa\left(\mathbf{r}\right)}{\mu_0}\mathbf{B}\left(\mathbf{r}\right), \tag{3.4}$$

where κ is the magnetic susceptibility. Combining eqs (3.3) and (3.4) yields

$$\mathbf{m}_j\left(\mathbf{r}_j\right) = \frac{\kappa_j}{\mu_0}\mathbf{B}\left(\mathbf{r}_j\right) \; w_j \; h_j. \tag{3.5}$$

Both the surface area, w_j, which is given by the chosen dipole distribution, and the inducing field, $\mathbf{B}$, taken from SH degree 1–15 of the CHAOS model, are known. The dipole moment strengths are determined from the observed induced field; their direction is given by that of the inducing field. Two unknowns, namely the susceptibility of the crustal rocks, κ_j, and the thickness of the magnetic crust, h_j, remain.

In order to solve for magnetic crustal thickness, knowledge of the susceptibility is required. The susceptibility of crustal rocks depends on material and temperature and is in general a second-order symmetric tensor. Most crustal rocks have slightly anisotropic magnetic susceptibilities. However, when considering the bulk properties of a large volume of rock the effective susceptibility is generally nearly isotropic and can therefore be treated as a scalar (Clark & Emerson, 1991). The temperature dependence of κ primarily results in variation of susceptibility with depth; in particular, κ approaches zero as the temperature approaches the Curie temperature. However, it is extremely difficult, if not impossible, to determine the vertical variation of the susceptibility from satellite data (e.g., Mayhew, 1982b; Mayhew *et al.*, 1991; Langel & Hinze, 1998, p. 119); only the depth integrated magnetization may be determined.

From crustal field models, such as MF5 (Maus *et al.*, 2007), it is evident that the crustal field is generally stronger over continents compared to over oceans. Although there is a tendency for the mafic oceanic rocks to have a slightly higher susceptibility than felsic continental rocks, due to a higher content of iron, magnesium and titanium (Clark & Emerson, 1991), the range of susceptibility values for continental and oceanic rocks overlap to a large extent. Thus, the stronger crustal field over the continents, compared to over the oceans, reflects the larger average thickness of the continental crust (about 40 km (Christensen & Mooney, 1995)) compared to the oceanic crust (about 7 km (White *et al.*, 1992)). Consequently crustal thickness plays an important role for the value of the depth integrated magnetization. Within continental crust lateral variation in susceptibility due to variations in geology is likely also to play an important role. However, for our purpose of applying this method to Greenland to infer magnetic crustal thickness and geothermal heat flux we are faced the problem of having

almost no knowledge of the geologic variations underneath the ice. Thus we make the assumption that the susceptibility is constant in continental crust and oceanic crust with values of $\kappa = 0.035$ SI and $\kappa = 0.040$ SI respectively (Schlinger, 1985; Purucker *et al.*, 2002). In order to include the continental shelf as continental crust, the division between oceanic and continental crust is taken to be where bathymetry exceeds 800 m. We also assume that the susceptibility is constant with depth down to the Curie depth where it becomes to zero.

Under the assumption of isotropic susceptibility the magnetic field caused by a large number of dipoles can be calculated through matrix multiplication. Let $\mathbf{b}$ be the vector of the radial, A_r, and southward, A_θ, components of the magnetic field at the observation points, $\mathbf{r}_i$ for $i =$ 1,2, ..., N,

$$\begin{aligned} \mathbf{b} &= \left(A_r\left(\mathbf{r}_1\right), A_r\left(\mathbf{r}_2\right), \cdots, A_r\left(\mathbf{r}_N\right),\right. \\ &\quad \left. A_\theta\left(\mathbf{r}_1\right), A_\theta\left(\mathbf{r}_2\right), \cdots, A_\theta\left(\mathbf{r}_N\right)\right)^T \end{aligned} \tag{3.6}$$

and let $\mathbf{d}$ be the magnitudes of the dipole moments of dipole $j = 1,2, \ldots, J$, then

$$\mathbf{b} = \mathbf{G}\mathbf{d}, \tag{3.7}$$

where the elements of the matrix $\mathbf{G}$ depend on the locations of the observation points, of the dipole locations, and of the direction (inclination and declination) of the main field.

Solving for the dipole moments of the crustal dipoles from the observed induced field is the inverse of the problem stated in eq. (3.7). However, as $\mathbf{G}$ is badly conditioned, a direct inversion is unlikely to provide a reasonable solution so we take an iterative forward approach. A scheme of this process is shown in Fig. 3.1.

To start the iterative procedure, an initial model of the magnetic crustal thickness is needed. We have used two different initial models; CRUST2.0 (Bassin *et al.*, 2000) and 3SMAC (Nataf & Ricard, 1996). CRUST2.0 is a seismic crustal model based on seismic data extending more than 40 years back, as well as on sediment and ice thickness compilations. It provides globally the thicknesses of seven layers: ice, water, soft sediments, hard sediments, upper crust, middle crust and lower crust, on a 2°×2° grid. As an initial magnetic crustal thickness model we combined the thicknesses of the upper, middle and lower crust. We do not include the sediment layers as these tends to have a significantly lower magnetic susceptibility than the crystalline rocks (Clark & Emerson, 1991) and thus are not included in the magnetic crust.

Similarly 3SMAC (Nataf & Ricard, 1996) was designed to provide a good crustal model to be used in global seismology. Besides seismic data, it is based on other geophysical data such as heat flow measurements, geological and geochemical data. Crustal thicknesses are provided on a 2°×2° grid, but only 4 layers (instead of 7 as for CRUST2.0) are given: water or ice, sediments, upper and lower crust. The division of upper and lower crust is made such that the upper crust constitutes 1/3 of the igneous crustal thickness up to a maximum of 20 km, the rest of the igneous crust is defined as lower crust. From 3SMAC we use the combined thickness of the upper and lower crust combined with information from the available geotherms to calculate a starting thickness of the magnetic crust (Purucker *et al.*, 2002). Compared to just using layer thicknesses, including the temperature information reduces the thickness of the initial model in the Himalayas and Andes. The inital crustal thickness model based on 3SMAC is shown in Fig. 3.2.

Since the CHAOS/MF5 crustal field model only consists of spherical harmonic degrees above 15, it can only constrain the short-wavelength variation of the magnetic crustal thickness. We

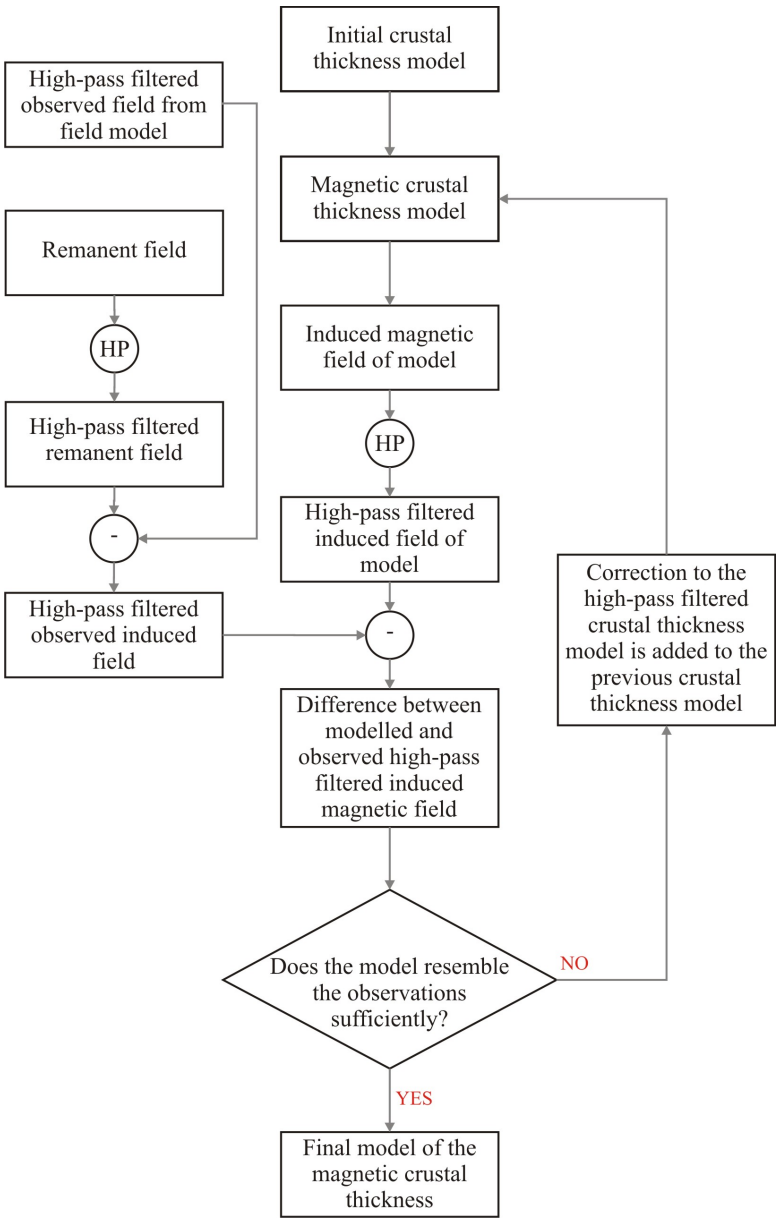

Figure 3.1: Iteration scheme. The various steps of the iteration procedure are explained in the text. HP: High-pass filtering.

therefore add the long-wavelength part of the initial model to our solution and iteratively only solve for the short-wavelength part (degrees > 15) of the magnetic crustal thickness from CHAOS/MF5.

In the forward modelling procedure the crustal dipole moments are calculated from the initial model of the magnetic crustal thickness. From these the induced crustal field is calculated using the ESMD method and high-pass filtered using a spherical harmonic transform. Then the high-pass filtered observed and modelled induced fields are compared. If their difference is large a new iteration is started and the crustal thickness model is improved: A correction to the initial model of the dipole moments is estimated by inversion of a sparse version of eq. (3.7) using a least squares conjugate gradient method (Purucker *et al.*, 1996). The inversion is done with a sparse version of the **G**-matrix to reduce the number of computations. In the sparse matrix only dipoles lying within a distance of 2500 km from a given observation point contribute to the field. Therefore more than 96% of the matrix elements are set to zero. The

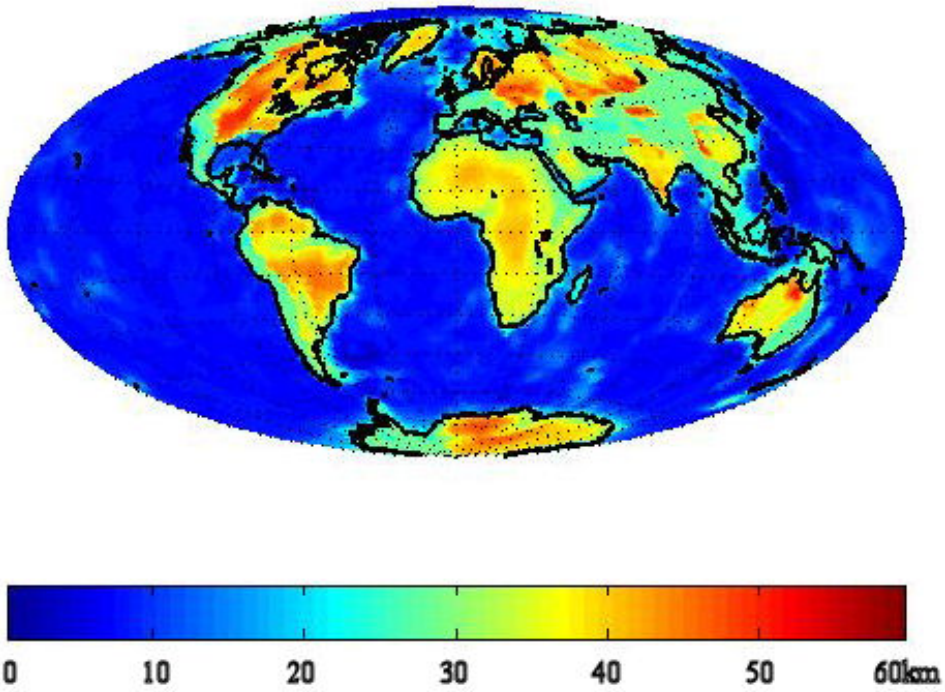

Figure 3.2: The crustal thickness based on 3SMAC which is used as initial model in the iterative procedure to determine the magnetic crustal thickness.

iteration is terminated once the magnetic crustal thickness model has stabilized and the solution appears reasonable in that it neither is too smooth nor too rough, this typically occurs in less than 10 iterations.

3.1 Results for the magnetic crustal thickness

We have solved for the magnetic crustal thickness using CRUST2.0 or 3SMAC as initial models for the crystalline crustal thickness. The result for the magnetic crustal thickness using 3SMAC is displayed in Fig. 3.3. We have chosen to show the result of 3SMAC because it is in slightly better agreement with other independent estimates of the magnetic crustal thickness (Artemieva, 2006) confirming the observation of Hemant & Maus (2005). The magnetic crustal thickness (of both initial models) displays oscillating behaviour in the vicinity of the magnetic equator, primarily in the region with inclination between -20° and 20°. We therefore refrain from interpreting the results in this area. We find that the magnetic crustal thickness is typically between 30 and 50 km in continental areas, although both higher and lower values occur.

Recently, Artemieva (2006) made a global 1°×1° thermal model, TC1, of the continental crust, based on a comprehensive data set of borehole heat flow data and information on local geologic age and tectonic settings. The gathered information was used to constrain continental geotherms in regions where reliable heat flow data are available, which is about 40% of the continental crust (Artemieva & Mooney, 2001; Artemieva, 2006); then extrapolation was done to the remaining continental crust by assuming that the same geotherms applies to areas with similar tectonic settings and age. TC1 provides a Curie depth map (Artemieva, 2006), which constitutes an opportunity for comparing our results with independent results based on a completely different data set. To obtain the Curie depth from

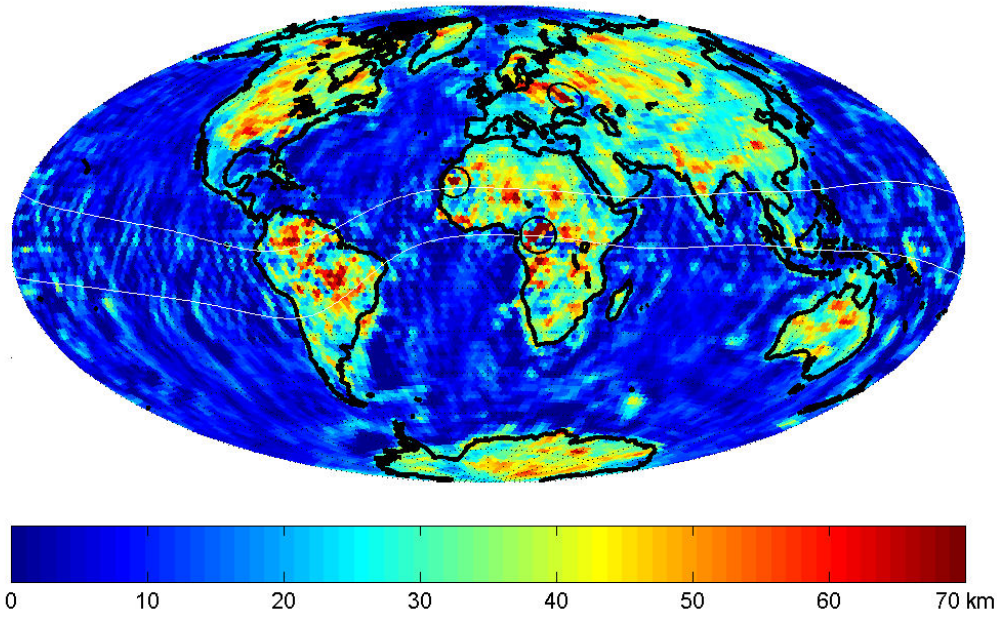

Figure 3.3: The magnetic crustal thickness derived from CHAOS/MF5 using 3SMAC as initial model (see Fig. 3.2). The white lines indicate the area around the magnetic equator with inclination between -20° and 20°. Three magnetic anomalies, which are discussed in the text, are indicated with black circles: Bangui (∼3°N,17°E) and Amsaga (∼21°N,12°W) in Africa and Kursk in Russia (∼51°N,38°E).

the magnetic crustal thickness, we add the thickness of the sediment layer (Laske & Masters, 1997; Bassin *et al.*, 2000). This Curie depth estimate only applies to the continental crust; in the oceanic crust, the lower boundary of the magnetic crust is expected to be Moho and thus does not represent the Curie depth. Similarly, the Curie depth estimate is erroneous in continental areas where Moho constitutes the lower boundary of the magnetic crust. As the sediment layer is less than a few kilometres thick in widespread continental areas our Curie depth map is very similar to our magnetic crustal thickness map.

In general we find reasonable agreement between TC1 and our Curie depth map. Both find the Curie depth typically at 30 km to 50 km depth; our Curie depth estimate has, however, a much higher variability compared to TC1. In most of the North American continent we find values similar to those predicted by TC1: below 40 km along the west coast and in Alaska and Central America, and predominantly between 40 and 60 km in the remaining North American continent. In the Scandinavian peninsula, we find Curie depths predominantly at 40–50 km, similar to TC1; in the Western Gneiss Region of western Norway we find the magnetic crustal thickness to become thinner at about 30–40 km, possibly reflecting Moho depth in this region (Kinck *et al.*, 1993). We also find good agreement in most of Australia, which will be treated in some detail later.

There are however, also some differences between the Curie depths of TC1 and our model, particularly in late Archean terranes (Artemieva, 2006), where TC1 generally predicts very large Curie depths. One such area is in Canada to the east and northwest of Hudson bay; here TC1 predicts the Curie depth to be more than 80 km, in the same area our model gives 50–60 km to the east and 40–50 km northwest of Hudson Bay. We believe that the discrepancy is due to Moho being shallower than the Curie isotherm in this area (Nataf & Ricard, 1996; Bassin *et al.*, 2000). As TC1 is based on data of heat flow, which are very low

in this area (Jaupart and Mareschal, 1999; Mareschal & Jaupart, 2004), TC1, probably correctly, predicts very large Curie depths in these areas. Another Late Archean area is in the central Fennoscandian Shield (in Finland), where TC1 yields large Curie depths of 50–70 km based on tectonic age and low measured heat flow (Artemieva, 2006), whereas our model predicts a rather thin magnetic crust (20–30 km). Our result does not reflect Moho depth, which is about 50 km in this region (Kinck *et al.*, 1993). A recent study on the lithology concludes that crustal composition in this region is more mafic than the average continental crust (Kuusisto *et al.*, 2006), which would indicate an above average susceptibility in this area. Thus a possible explanation for our underestimate of the magnetic crustal thickness in this area is the presence of remanent magnetization in the crust.

At some locations, namely in connection with strong magnetic anomalies, unusual or odd results of the magnetic crustal thickness are to be expected. One example is the Bangui anomaly in Africa, which is believed to be caused by anomalously high susceptibility values in the lower crust, due for example to a mafic composition, or by remanent magnetization, or perhaps by a combination of both (Ravat *et al.*, 2002; Hemant & Maus, 2005). In either case our method does not account for these anomalous conditions and therefore produces unrealistic results in this area; specifically our model predicts an area of very thick magnetic crust right next to an area with negative magnetic crustal thickness. A second famous magnetic anomaly is Kursk. In this area our model predicts a very thick magnetic crust, which probably is not the case here (Artemieva, 2006). Remanent magnetization is a likely cause of the Kursk magnetic anomaly (Hemant & Maus, 2005), which could cause our model to overestimate the magnetic crustal thickness in this area. We also find very thick magnetic crust in the Amsaga Shield in Africa, but this may well be a valid result here (Hemant & Maus, 2005; Artemieva, 2006). It is possible that magnetization extends into the upper mantle (Toft & Haggerty, 1988; Toft *et al.*, 1992), but the magnetic anomaly could also be due to above average magnetization of the lower crust (Hemant & Maus, 2005) in this region.

Since we later estimate heat flux from the derived Curie depths in Australia and Greenland, we have plotted maps of the Curie depths in these regions in Fig. 3.4 and 3.5 respectively, and will discuss these areas in some detail.

3.1.1 Australia

The Australian continent is broadly divided into three large-scale tectonic areas; the Archean West Australia, the Proterozoic Central Australia, and the Phanerozoic East Australia. We find that the magnetic crust is relatively thin (20–30 km) in most of East Australia, a bit less than the 30–40 km TC1 suggests. In the rest of Australia, we find the magnetic crust to be predominantly 30–50 km thick compared to 40–50 km in TC1. One noticeable exception is an area in the southeast of West Australia, where our model predicts thin magnetic crust, which we discuss below.

To evaluate whether the magnetic crustal thickness in Australia reflects the depth to Moho, or the Curie depth, we have compared the obtained Curie depth map with seismic determined Moho depths (Collins, 1991; Shibutani *et al.*, 1996; Clitheroe *et al.*, 2000). We find that the lower boundary of the magnetic crust clearly lies shallower than Moho in eastern Australia, whereas it appears that they are roughly equal elsewhere. This implies that the lower boundary of the magnetic crust in eastern Australia is given by the Curie isotherm, whereas it may be given by Moho elsewhere in Australia.

We also compared our magnetic crustal thickness with a temperature model of the upper

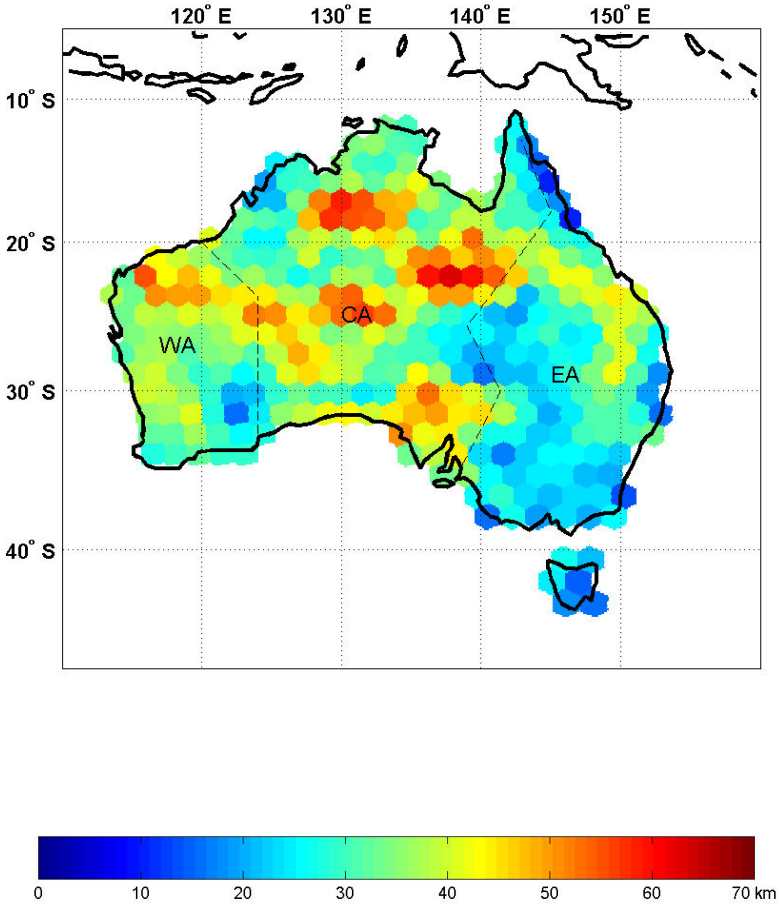

Figure 3.4: The estimated Curie depth from CHAOS/MF5 using 3SMAC as initial model. The dashed lines indicates the division of Australia into East Australia (EA), Central Australia (CA) and West Australia (WA).

Australian mantle by Goes *et al.* (2005), who derived two maps of the temperature at 140 km depth based on two different seismic models of the upper mantle by various authors. They find higher temperature at 140 km depth in eastern Australia, compared to the rest of the continent, and similar temperature ranges in West Australia and Central Australia, although the temperature varies considerably within both regions. Our estimate of the Curie depth is in agreement with this pattern, confirming that our method provides a robust estimate of the thermal conditions at depth. The geotherms presented by Goes *et al.* (2005) indicate that the temperature may not reach 580°C until about 80 km depth in the West Australia. This is much deeper than Moho (Clitheroe *et al.*, 2000) indicating that Moho defines the lower boundary of the magnetic crust in this region.

The predicted low magnetic crustal thickness in the southeast of West Australia is surprising; in this area, which is predominantly early Archean (Artemieva, 2006), TC1 predicts a very large Curie depth of 60–70 km based on measured low heat flow (Cull, 1991; Artemieva, 2006). Neither CRUST2.0 nor 3SMAC has a local low here, thus the result of low magnetic crustal thickness here must origin from either the field model, the presence of remanent magnetization, or a below average susceptibility. Using several different field models (MF3, MF4 (Maus *et al.*, 2006), MF5 (Maus *et al.*, 2007) and CM4 (Sabaka *et al.*, 2004)) as input for our method we found that the thin magnetic crust in this area is a robust feature. This

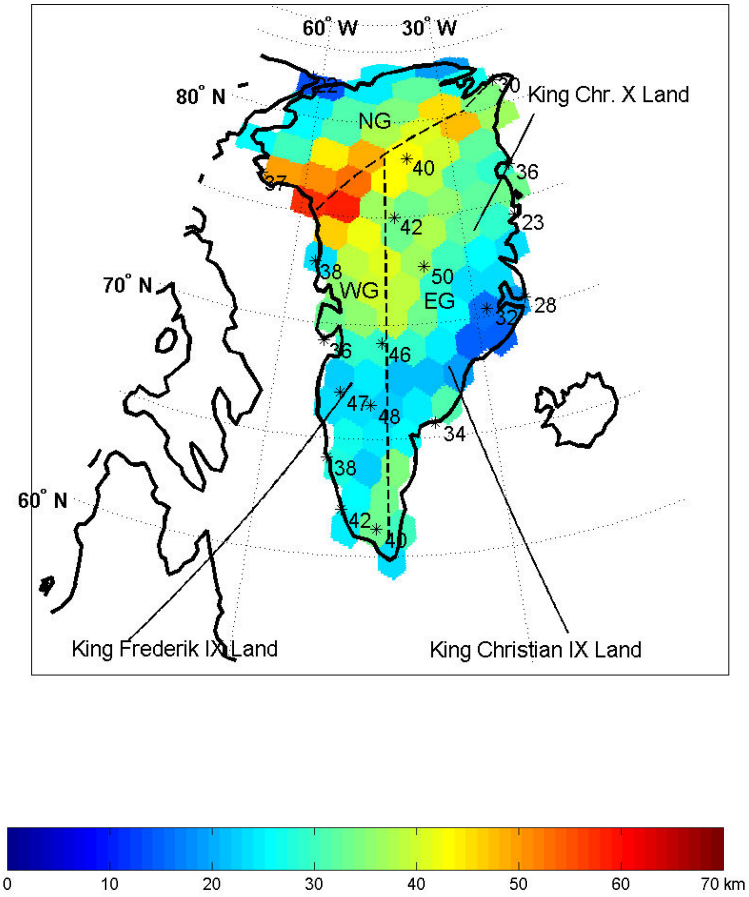

Figure 3.5: The estimated Curie depth from CHAOS/MF5 using 3SMAC as initial model. The dashed lines indicates the division of Greenland into East Greenland (EG), West Greenland (WG), and North Greenland (NG). The black stars show the Moho depths by Dahl-Jensen *et al.* (2003b).

also holds whether 3SMAC or CRUST2.0 is used as initial model. The reason for this discrepancy is unclear to us, but we consider either low susceptibility or subsurface remanent magnetization to be possible causes.

3.1.2 Greenland

Our second key area of interest is Greenland. Here we find large Curie depths of 50–60 km on the border of North and West Greenland. Extending from that area along the border between North and East Greenland, and somewhat southwards along the border between East and West Greenland the Curie depth is 40–50 km. In most of the remaining part of the northwestern half of Greenland the Curie depth is 30–40 km, whereas it is 20–30 km in most of the southeastern half. Most noticeably we find the Curie depth in the coastal area between King Christian IX and King Christian X land to be less than 20 km. Using both a suite of different field models and the two different initial models, we found these features of the magnetic crustal thickness to be very robust.

There appears to be a dividing line between relatively thick magnetic crust (30–60 km) in northwestern Greenland and relatively thin magnetic crust (10–30 km) in southeastern

Greenland. This dividing line coincides remarkably well with the boundary between two distinct Proterozoic blocks proposed by Dahl-Jensen *et al.* (2003b) based on seismic experiments. A recent study by Hemant & Maus (2005) supports such a division. Interestingly though Dahl-Jensen *et al.* (2003b) proposed the division based on a generally deeper lying Moho discontinuity in southeast Greenland compared to northwest, whereas we find the magnetic crust to be thicker in northwest compared to southeast Greenland. However, the observation of generally stronger crustal magnetization in the northwestern compared to the southeastern block appears to be consistent (Hemant & Maus, 2005), and thus we consider the magnetic crustal thickness estimate realistic.

Again, we compare our Curie depth estimate with local Moho determinations to evaluate if Moho or the Curie isotherm constitutes the lower boundary of the magnetic crust. Based on local seismic data, Dahl-Jensen *et al.* (2003b) determined the depth to Moho at 19 locations in Greenland. We find that the magnetic crustal thickness is less than the depth to Moho at all locations, except at (78°N,39°W) (Gregersen *et al.*, 1988), where we find similar values. It thus appears that the Curie depth is shallower than Moho in most of Greenland. In particular, we note that the Curie depth is shallower than Moho in the central part of East Greenland, where additional seismic studies have been made (Mandler & Jokat, 1998).

We have compared our Curie depth map for Greenland, with the Curie depth map of TC1 (Artemieva, 2006). There are rather large deviations between our result and TC1, but this is not surprising. TC1 estimates the Curie depth to be about 40–50 km in most of Greenland, with somewhat lower values (30–40 km) along the east coast, and with somewhat larger values (50–60 km) in King Frederik IX Land and the surrounding area based on the presence of an early Archean craton in south Greenland. With very few direct heat flow measurements in Greenland and very limited information on the surface and deep geology underneath the ice, TC1 is less constrained in Greenland compared to most other areas. Based on a field model our result is equally constrained everywhere, making the estimate of the magnetic crustal thickness and thus the Curie depth as reliable here as elsewhere.

3.1.3 Difference between 3SMAC and CRUST2.0

The difference between the resulting magnetic crustal thickness using 3SMAC or CRUST2.0 as initial model is the same as the difference between the long-wavelength variation of the two shown in Fig. 3.6. This demonstrates that the derived short-wavelength variation of the magnetic crustal thickness is completely determined by the field model, whereas the long wavelength variation of the magnetic crust thickness is completely unconstrained. For the long wavelength features, 3SMAC gives in general slightly higher (∼2 km) values of the magnetic crustal thickness than CRUST2.0 in oceanic areas, whereas CRUST2.0 gives higher values than 3SMAC in continental areas. In particular in the Himalayas and most of Asia, CRUST2.0 gives much higher values ($\geq$ 10 km) than 3SMAC, but this is due to the reduction in thickness of 3SMAC mentioned in Sec. 3.

4. Thermal model of the crust

We also investigated whether it is possible to estimate the geothermal heat flux from the obtained Curie depths. This requires a thermal model of the crust, i.e. the theoretical prerequisites for modelling the temperature in the crust. We need a thermal model which reflects the condition of the continental crust between the surface and the lower boundary of the magnetic crust. In this region the dominant heat transfer mechanism is heat conduction.

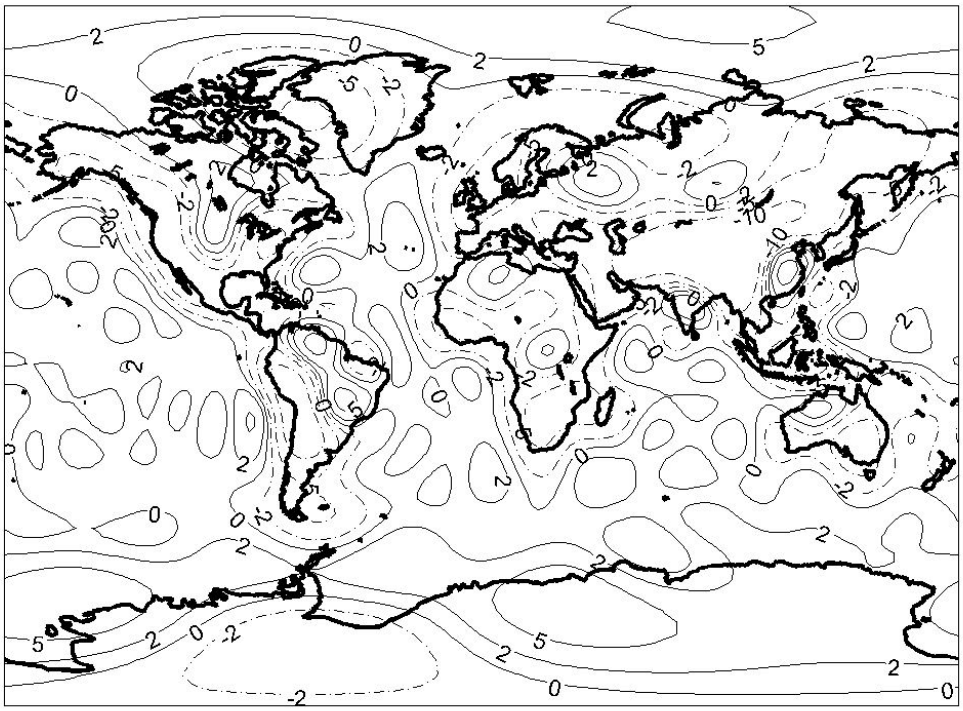

Figure 3.6: The difference between the low pass filtered igneous crustal thickness of 3SMAC and the low pass filtered thickness of the crystalline crust of CRUST2.0. Contour lines are drawn at 0 km, ±2 km, ±5 km, and ±10 km. Positive values (solid lines) are where 3SMAC has higher values than CRUST2.0; negative values (dashed lines) are where 3SMAC has lower values than CRUST2.0.

As vertical temperature gradients in general dominate horizontal gradients in the continental crust, we use the one-dimensional heat conduction equation to model heat transfer. In addition we assume steady state; as no time dependent data are available, it is not possible to resolve temporal changes. In stable cratonic crust this assumption is probably reasonable as thermal equilibrium may have been reached, but in recently tectonically active areas this assumption may be violated, as transient effects may still influence the thermal state of the crust.

Two parameters significantly influence the thermal state of the crust: crustal heat production and thermal conductivity. The heat production is the least constrained, and thus most difficult, parameter to handle when attempting to make a thermal model of the continental crust. Heat production by decay of radioactive elements varies significantly both laterally and vertically. As the heat production varies so does its contribution to the heat flux, but it is generally large; 30–60% or even more of the surface heat flux is due to crustal heat production (Kremenetsky *et al.*, 1989; Kukkonen & Lahtinen, 2001; Brady *et al.*, 2006), which makes it a very important parameter in any thermal model of the crust. Several studies have shown that the heat production predominantly varies with lithology (e.g. Jaupart and Mareschal, 1999; Kukkonen & Lahtinen, 2001; Mareschal & Jaupart, 2004; Senthil Kumar & Reddy, 2004). However, it also varies within a given rock type (Senthil Kumar & Reddy, 2004; Abbady *et al.*, 2006); rock type is determined by the bulk composition of a given rock, whereas heat production is determined by trace elements. This means that for example seismic studies cannot be used to infer heat production (Kukkonen & Lahtinen, 2001), because the seismic properties of a rock are independent of its trace elements.

The heat production is generally believed to be higher in the upper crust compared to the middle and lower crust (Kukkonen & Lahtinen, 2001; Sandiford & McLaren, 2002; Abbady *et al.*, 2006; Brady *et al.*, 2006). Heat producing elements can be redistributed in the crust by processes such as erosion, sedimentation, deformation and partial melting. In particular, the latter is thought to cause an upward concentration of heat producing elements, as they readily enter the melt and rise towards the surface along with the magma. But even small changes in the rock forming process can significantly alter the amount of heat producing elements in the resulting rock. The detailed variation of heat production with depth is therefore difficult to determine. There are two main approaches to do this; either in boreholes (e.g. Kremenetsky *et al.*, 1989), which gives the present vertical variation, or at exposed crustal sections where the past heat production profile may be determined (e.g. Ketcham, 1996; Senthil Kumar & Reddy, 2004; Brady *et al.*, 2006). Such studies have shown that there is a general tendency of decreasing heat production with depth, but that local deviations from this may occur and that variation with depth is neither smooth nor systematic. Other studies have found no systematic dependency of crustal heat production on crustal age (Jaupart and Mareschal, 1999; Kukkonen & Lahtinen, 2001) and so far there is no indirect method to determine the variation of heat production at depth over large areas.

Thermal conductivity is in general a second order tensor however, for many types of rocks, particularly volcanic and plutonic rocks, it is isotropic and can be treated as a scalar (Clauser & Huenges, 1995). The conductivity is material dependent, i.e. it varies with geology, and may vary by more than a factor of two for a given rock type due to changes in for example porosity, degree of saturation, temperature, pressure, dominant mineral phase, and quartz content (Clauser & Huenges, 1995; Kukkonen *et al.*, 1999). The most pronounced systematic behaviour of conductivity with depth is its temperature dependency. Conductivity varies linearly with inverse temperature and thus decreases with increasing temperature, i.e. depth (Durham *et al.*, 1987; Clauser & Huenges, 1995; Kukkonen *et al.*, 1999).

The unanimous conclusion of the many studies of the depth variation of heat production and of thermal conductivity mentioned above, is that the variation of these parameters is not systematic, and thus cannot be described or modelled in any simple way. Both parameters vary primarily with lithology, but large scattering occurs for a given lithology. The lack of systematic variability and of methods to estimate the intra crustal heat production and conductivity means that ideally empirically determined depth profiles based on local measurements should be applied in any thermal model of the crust. However, as measurements of the present depth variation of heat production and conductivity are very scarce, this is not feasible in practice. The current tendency is to divide the crust into a large number of different crustal types based on geologic, tectonic, lithologic, and seismic information and then assign individual heat production and conductivity profiles to each crustal type; this is the approach taken in TC1 (Artemieva, 2006). It appears to work well, but is limited to areas where the necessary information about the crustal type is available. As our aim is to estimate the heat flux in an ice-covered area, where lithologic information is not available, we have to make a much more crude model of the thermal properties of the crust independent of such information.

Inspired by the heat production and thermal conductivity studies cited above, we make a 4-layer thermal model of the crust (Artemieva & Mooney, 2001; Kukkonen & Lahtinen, 2001; Artemieva, 2006), in which the crust is divided into sediments, upper crust, middle crust and lower crust. Layer thicknesses are adopted from CRUST2.0 as 3SMAC does not include a middle crust layer. The thermal properties of each layer are assigned separately. In the

sediment layer, if present, the conductivity and heat production are assumed constant (Artemieva & Mooney, 2001; Kukkonen & Lahtinen, 2001; Artemieva, 2006). In the upper crust, the thermal conductivity is assumed to vary linearly with inverse temperature (e.g. Durham *et al.*, 1987; Clauser & Huenges, 1995; Ketcham, 1996; Kukkonen *et al.*, 1999); following Artemieva & Mooney (2001) and Artemieva (2006), we use

$$k\left(T\right) = \frac{k_0}{1 + 0.001T} \tag{4.1}$$

where T is the temperature in °C and k_0 is the conductivity at $T = 0$°C. The heat production in the upper crust is also assumed to decrease with depth, again we follow Artemieva & Mooney (2001) and Artemieva (2006) and use

$$H\left(z\right) = H_0 \exp\left(-\frac{z}{\delta}\right), \tag{4.2}$$

where H_0 is the heat production at the top of the upper crust, z is the depth, and δ is the scale depth at which the heat production has decreased to $1/e$ (=0.368) of H_0. The decrease of crustal heat production with depth is known not to be exponential (e.g. Ketcham, 1996; Jaupart and Mareschal, 1999; Mareschal & Jaupart, 2004; Abbady *et al.*, 2006; Brady *et al.*, 2006), but no good alternative has been presented to model the decrease with depth. Also we stress that this approximation is used only for the upper crust. In the middle and lower crust the conductivity and heat production are assumed constant in each layer, but both are higher in the middle compared to the lower crust.

We numerically solve the heat conduction equation

$$\frac{\partial}{\partial z} k\left(T\left(z\right)\right) \frac{\partial T\left(z\right)}{\partial z} = -H\left(z\right), \tag{4.3}$$

specifying two boundary conditions: the temperature at the surface (i.e. at the top of the sediments) is 0°C and the temperature at the Curie depth is 580°C. We solve for the temperature profile iteratively. First an initial model for the temperature is assumed from which the conductivity profile is calculated. Then a new temperature profile is calculated from the given conductivity and heat production profile. With the new temperature profile, an adjusted conductivity profile is determined from which a new temperature profile is calculated etc.. The iteration is continued until the change of the temperature in each nodepoint is less than 10^{-5} K between two consecutive iterations. The temperature profile of the crust is calculated using a 20 m vertical grid spacing if the Curie depth of a crustal block is less than 45 km, and with a grid spacing of 20 m in the upper 20 km and 40 m below this, if the Curie depth is more than 45 km. Note that the boundary conditions we specify are temperatures; we do not make assumptions regarding the amount of mantle heat flow and thus cannot make statements on the partition of contributions to the surface heat flux from crustal heat production and mantle heat flow.

Once the temperature profile has been determined, the heat flux is calculated as the average heat flux in the top 100 m of the crust (top 5 grid points). This averaging is done to avoid a large impact on the heat flux result by a thin sediment layer ($\leq$20 m), which for example is present in large parts of Greenland (Laske & Masters, 1997; Bassin *et al.*, 2000).

To estimate the values of the thermal parameters that enter into the 4-layer thermal model, we apply the model to Australia using the estimated Curie depth. We adjust the thermal parameters one by one and compare the outcome for the heat flux with the heat flow map of

TC1 (Artemieva & Mooney, 2001; Artemieva, 2006). Based on the best fit, we take the thermal conductivity, k of the sediment layer and of the middle crust to be 2.2 W/mK and of the lower crust to be 2.0 W/mK, in the upper crust we use $k_0 = 2.9$ W/mK (Clauser & Huenges, 1995; Ketcham, 1996; Kukkonen *et al.*, 1999; Artemieva & Mooney, 2001). For the heat production we take 1 μW/m^3 in the sediment layer, 0.3 μW/m^3 in the middle crust and 0.15 μW/m^3 in the lower crust, in the upper crust we use $H_0 = 4.5$ μW/m^3 and $\delta = 8$ km (Ketcham, 1996; Artemieva & Mooney, 2001; Kukkonen & Lahtinen, 2001; Abbady *et al.*, 2006; Brady *et al.*, 2006).

4.1 Results for the geothermal heat flux

We have applied the thermal model to two areas. Australia, as a reference area, where our model results can be compared to direct heat flux measurements, and Greenland, an area where a heat flux map is desirable for, for example ice sheet modelling, but where direct measurements are extremely laborious and costly to make.

4.1.1 Australia

The result for the heat flux in Australia is shown in Fig. 4.1. We find elevated heat flux in most of East Australia, in particular in the western part of East Australia, and a local minimum in the eastern part of East Australia. In Central Australia we find intermediate heat flux values in the southern half, and alternating above and below average values in the northern part in an east-west trending pattern.

These regional variations in East and Central Australia match quite well those of TC1 (Artemieva, 2006). The variation pattern is somewhat better reproduced than the absolute values. Compared to TC1, we slightly underestimate the absolute values in East Australia, where we find heat flux of 70–90 mW/m^2, compared to 80–110 mW/m^2 from TC1. The intermediate values of 50–60 mW/m^2 that we find in the southern half of Central Australia are similar to those of TC1. At the South Australian heat flow anomaly ($\sim$32°S, 138°E) on the border of East and Central Australia, we underestimate heat production, which has been estimated to be two to three times larger than that typical for Proterozoic crust (Neumann *et al.*, 2000).

In the southeastern corner of West Australia our method predicts a large region of elevated heat flux, this is due to the shallow Curie depth that our method predicted here. As already discussed we do not think the estimated shallow Curie depth reflects the true value, and thus do not consider the heat flux estimate here realistic. The area is in fact known to have low heat flow of 30–50 mW/m^2 (Cull, 1991; Artemieva, 2006). Besides the erroneous Curie depth values used here, our model may also be assuming overly high crustal heat production in West Australia, where it is actually likely to be below average. We find an average heat flux in Australia of 64 mW/m^2, which is close to the average of the continental crust of 65 mW/m^2 (Pollack *et al.*, 1993).

In addition to comparing with TC1, we have compared our results with a global heat flux map derived by Shapiro & Ritzwoller (2004), who used a global seismic model to extrapolate heat flux measurements to areas where no measurements are available based on structural similarity. They assume that crustal heat production is similar in regions with similar crustal structure, which is a somewhat similar approach to ours, and their spatial resolution is also similar to ours, making a comparison favourable. Shapiro & Ritzwoller (2004) find elevated heat flux of 70–90 $\pm$ 50 mW/m^2 in East Australia, whereas they find average heat flux of 50

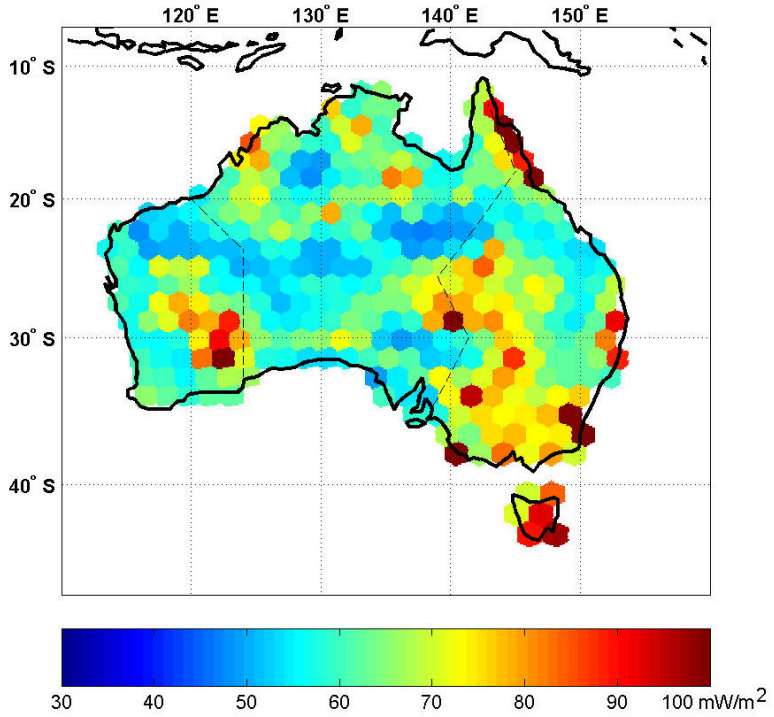

Figure 4.1: The geothermal heat flux in Australia. We find elevated heat flux in most of East Australia, and intermediate values in most of Central Australia.

$\pm$ 20 mW/m^2 in the remainder of Australia: this is coherent with our results for Australia, apart from the anomalies discussed in parts of West Australia.

The Moho depth determinations (Clitheroe *et al.*, 2000) and the temperature depth map (Goes *et al.*, 2005) lead to the conclusion that the Curie isotherm constitutes the lower boundary of the magnetic crust in East Australia, whereas Moho could be the lower boundary in Central and West Australia. The good agreement of our heat flux estimate and the heat flux map of TC1 in Central Australia indicates that the Curie isotherm also constitutes the lower boundary of the magnetic crust here. The poor estimate of the heat flux in West Australia could point to Moho being the lower boundary here, but as already discussed, the assumptions made regarding crustal heat production and magnetic susceptibility may be violated in this region, leading to an anomalous result.

4.1.2 Greenland

Based on the good agreement of our heat flux estimate and TC1 in East and Central Australia, we are encouraged to apply the method to Greenland, where only a few heat flux measurements are available, and spatial heat flux variations are not easily obtained. Results are shown in Fig. 4.2. Heat flux is above average (60–80 mW/m^2) in and around King Christian IX Land and Frederik IX Land, particularly in the coastal area between King Christian X Land and King Christian IX Land where values are highest, reaching 90–110 mW/m^2. In the central part of North Greenland and halfway down West Greenland we estimate the heat flux to be 50–60 mW/m^2. On the border of North and West Greenland we find an area with heat flow less than 50 mW/m^2. We find the average heat flow in

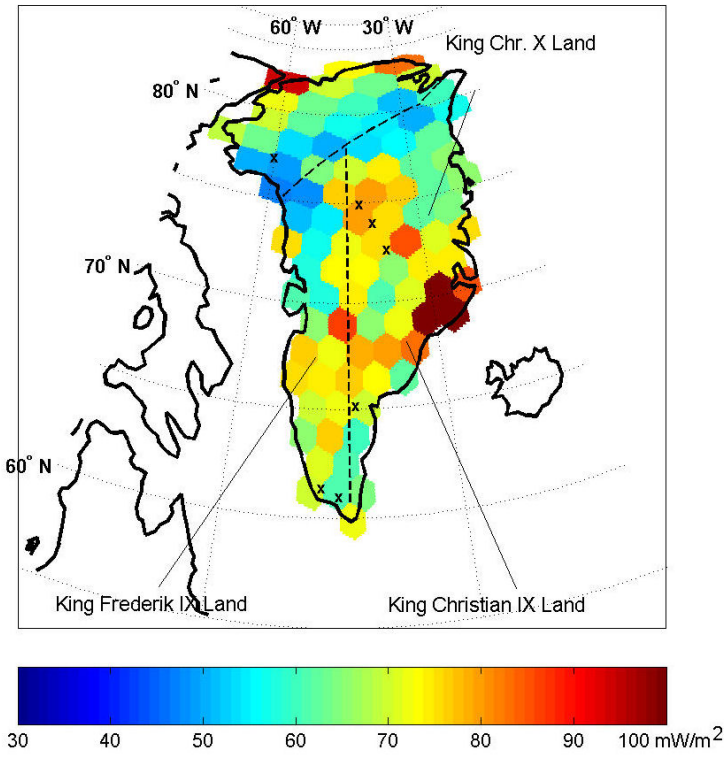

Figure 4.2: The geothermal heat flux in Greenland. We find below average heat flux in North Greenland, and above average heat flux in most of central Greenland. High heat flux is found in the central part of East Greenland. The x's mark the locations of independent local heat flux estimates mentioned in the text, from north to south: Camp Century, NGRIP, Fahnestock location, GRIP, Dye 3, Ivigtut and Ilímaussaq.

Greenland to be 68 mW/m^2 which is close to the continental average (Pollack *et al.*, 1993). Shapiro & Ritzwoller (2004) predict elevated heat flux of 70–90 $\pm$ 50 mW/m^2 along the southeast coast and in the southern tip of Greenland, and average heat flux of 50 $\pm$ 20 mW/m^2 in the remainder of Greenland; our results are coherent with this.

In Greenland, direct heat flux measurements have been made at a few coastal sites and in ice covered areas a handful of local heat flux estimates have also been made, using various methods. It is difficult to directly compare local values with a smoothed map as discrepancies are bound to occur, but it is nevertheless interesting to make the direct comparison.

Sass *et al.* (1972) measured values of heat flux, thermal conductivity and surface heat production at two sites in south Greenland (see Fig. 4.2); giving 42 mW/m^2, 2.8 W/mK and 2.3 μW/m^3, respectively, at Ivigtut. At Ilímaussaq, less than 100 km SSE from Ivigtut the heat flux was measured to be 37 mW/m^2, the thermal conductivity to be 2.3 W/mK, and the surface heat production to be 9.7 μW/m^3; the high heat production here is due to a local, highly radioactive intrusion (Sass *et al.*, 1972). The large difference in the surface heat production at these two fairly close sites illustrates the complex variability possible in Greenland. Our estimate of heat flux at these sites is about 60 mW/m^2. A possible explanation for the overestimate given by our method is that the crustal heat production is overestimated in this area. The surface heat production is very high at Ilímaussaq, but the intrusion carrying the high heat production is thin (Sass *et al.*, 1972) and the measured heat

flux here is below the continental average, so the actual total crustal heat production here is probably lower than the one assumed in our model.

At the Camp Century ice core drill site in northwestern Greenland (see Fig. 4.2) the heat flux has been estimated to be about 50 mW/m^2 (Gundestrup *et al.*, 1993; Greve, 2005); this is in agreement with the heat flux we find in this area, and corroborates a thick magnetic crust here. At the GRIP drill site (Fig. 4.2), the geothermal heat flux has been estimated to be 51 mW/m^2 by inversion of the temperature profile measured through the ice cap (Dahl-Jensen *et al.*, 1998). Here we find a higher heat flux of 75 mW/m^2; the discrepancy can be attributed to an overestimated crustal heat production in this area. The heat flux at Dye 3 (see Fig. 4.2) has been estimated to be 20 mW/m^2 (Gundestrup & Hansen, 1984; Dahl-Jensen *et al.*, 1998; Greve, 2005) but our method estimates a higher heat flux in this area. It is likely that the crustal heat production here is lower than assumed as a heat flux of 20 mW/m^2 indicates a very low crustal heat production.

At the NGRIP ice core site (Fig. 4.2) several estimates of the heat flux have been made ranging from 98 mW/m^2 to 140 mW/m^2 (Grinsted & Dahl-Jensen, 2002; Dahl-Jensen *et al.*, 2003a; North Greenland Ice Core Project members, 2004; Buchardt & Dahl-Jensen, 2006). Buchardt & Dahl-Jensen (2006) also estimated the heat flux along the ice flow-line leading to the NGRIP site 100 km upstream of NGRIP using radio-echo sounder observations. They found the heat flux to vary between 121 mW/m^2 and 231 mW/m^2, with an average value of about 155 mW/m^2. These values are very high for continental heat flux (Pollack *et al.*, 1993; Artemieva, 2006). The rather large variability of the heat flux along the flow line, where differences of more than 50 mW/m^2 occur between two neighbouring 4 km intervals on several occasions indicate a very shallow origin of a large amount of crustal heat production (Buchardt & Dahl-Jensen, 2006). We find the heat flux to be 70–80 mW/m^2 in this area; our somewhat lower value can be due to an underestimation of the crustal heat production in this area, particularly the shallow crustal heat production. But we stress that our heat flux value is given as the average value of an area of thousands of square kilometres; as some of the values obtained by Buchardt & Dahl-Jensen (2006) are very high, we speculate that these values are rather local, and that the surrounding area may have a lower heat flux, bringing the average of the crustal block down. In the TC1 3°×3° binned heat flow database, fewer than 3% of the crustal blocks have an average of more than 100 mW/m^3 indicating that such high heat flux rarely occurs over areas of this size. The map of Shapiro & Ritzwoller (2004) does not indicate a high heat flux in the NGRIP area either, which supports the idea that elevated heat flux here is most likely due to unusual crustal heat production at shallow depth.

Using airborne radar soundings to track internal layers in the ice, Fahnestock *et al.* (2001) estimated the melt rate of the basal ice along their flight track and found it to vary a great deal. At (∼74°N,40°W) (location marked in Fig. 4.2), they estimated the melt rate and thus the heat flux to be very high, more than 15 times the global average. Supported by bedrock topography and gravity they speculate that a volcano could be present under the ice here. At this site, we estimate the heat flow to be 70–80 mW/m^2; the discrepancy is again most likely due to the difference in resolution.

In summary we find a highly variable predicted heat flux in Greenland, in agreement with the other, rather limited studies conducted here. The absolute values we calculate are within typical heat flux values present in the TC1 heat flow data base. The agreement with the TC1 heat flux map in Australia indicates that our method reflects the heat flux variation at the given resolution. We attribute the differences between the local heat flux estimates at GRIP,

NGRIP and Dye 3 and our results in part to the high variability on short spatial scale that the heat flux may display and in part to variation in the intra-crustal heat production, which locally may be higher or lower than our assumed average model.

It is clear that the method of estimating the heat flux presented in this paper is based on numerous simplifying assumptions; regarding the thermal part of the model the most important one is the lack of variability of the crustal heat production with respect to lithology. However, application of the method to Australia reveals rather good results in spite of the obvious caveats of the applied heat production profile. It is nevertheless clear that the ideal would be to apply a lithology dependent heat production. Such information is challenging to obtain for ice covered regions, leaving the problem of mapping the spatial variation of the heat flux underneath the ice standing. The approach of estimating the heat flux by tracking isochrones in the ice detected by radar-sounding (e.g. Fahnestock *et al.*, 2001) has so far been done only along single tracks, but better coverage of such data in the future may give more accurate results. This method requires no assumptions or knowledge of the crustal heat production, but the ice flow model used to model the radar-layers in the ice depends on the spatial and temporal variability of the accumulation over the ice cap during tens of thousands of years. In addition, several heat sources and sinks exist at the ice-bed rock boundary including frictional heating, possible latent heat from melting or re-freezing at the bottom of the ice, heat conducted and advected through the ice in addition to the geothermal heat flux. To isolate the latter requires specification of all the other; thus this approach has a different set of deficiencies. As yet no ideal method to estimate the spatial variability of the heat flux under the ice sheets exists.

5. Discussion of errors

The method we have derived to determine the magnetic crustal thickness and estimate the heat flux has several sources of uncertainty, which must be evaluated to make an estimate of the uncertainty of the results.

The basis of the study is the crustal field model, in this case CHAOS/MF5 (Olsen *et al.*, 2006; Maus *et al.*, 2007). Errors in the field model will transfer directly into errors in the estimate of the magnetic crustal thickness. Although improvements occur continuously, and the data set used to derive field models also grows continuously, crustal field models still suffer from rather high uncertainty. Based on a recent study of error estimates of field models (Lowes & Olsen, 2004) we consider a conservative estimate of the uncertainty of the field model to be 20–25%.

The initial crustal thickness model also introduces errors in the magnetic crustal thickness estimate, more specifically into the long wavelength part of the solution as discussed in Sec. 3.1.3. Differences between the long wavelength crustal thickness of CRUST2.0 (Bassin *et al.*, 2000) and 3SMAC (Nataf & Ricard, 1996) rarely exceeds 5 km. Considering this difference as indicative of the possible error introduced by the initial model, we find that a difference of 5 km compared to the average continental crustal thickness of 42 km (Christensen & Mooney, 1995) corresponds to an error of 12%.

Unmodelled remanent magnetization comprises another source of error on the magnetic crustal thickness. Remanent magnetization in the continental crust may lead to erroneous estimates of the magnetic crustal thickness, as seen for Kursk and Bangui. Detailed maps of remanent magnetization in Greenland and Australia are not available, but no large remanent anomalies are immediately obvious from the observed crustal field. Furthermore our magnetic

crustal thickness for both Greenland and Australia are realistic in that they are neither very large nor negative, which indicates that remanent magnetization is not required to explain the observed crustal field here. It is difficult to quantify the error caused by unmodelled remanent magnetization, but the starting model (3SMAC), predicts the location and roughly the magnitude of 11 out of 14 regional magnetic anomalies in Greenland and Australia. Thus induced magnetization can explain about 80% of the observed crustal field. We therefore argue that the error due to unmodelled remanent magnetization is at most 20%.

Our derived magnetic crustal thickness depends linearly on the magnetic susceptibility. Since the crustal dipole moments are constrained by the field model, it is essentially the product of susceptibility and magnetic crustal thickness that is constrained. Thus a higher value of magnetic susceptibility results in a thinner magnetic crust and vice versa. The model we adopt for the magnetic susceptibility does not account for either lateral or vertical variation of susceptibility, except for the ocean-continent difference. Unfortunately, no global or regional maps of the magnetic susceptibility exist that are not constrained by satellite magnetic data and based on a priori assumptions about the magnetic crustal thickness. It is difficult to asses the error originating from making this assumption. Each crustal block in Greenland typically represents a volume between $2{\cdot}10^5$ km^3 and $12{\cdot}10^5$ km^3, if the average susceptibility of these block varies with 10% then the error due to the assumption made here will be 10%, but we recognize that it may be larger.

The assumptions of constant temperature at the top and bottom of the magnetic crust constitute an error source of the heat flux estimate. In Greenland the presence of the ice cap means that the bedrock temperature probably does not vary significantly, in time or geographically. The temperature under the ice is probably between 0°C and -30°C (Gundestrup & Hansen, 1984; Huybrecths, 1991; Gundestrup *et al.*, 1993). The situation in Australia is obviously different however, the range of the mean annual temperature is also at the 30 K level. Compared to the total temperature difference across the magnetic crust of 580 K, the variation in bedrock temperature constitutes only a minor source of error of about 5%. The uncertainty associated with the lower boundary temperature is of comparable size. The exact value of the Curie temperature depends on pressure and on the specific composition of the rock. According to Schlinger (1985) the Curie temperature of lower crustal rocks varies between 550°C and 580°C. This therefore also constitutes an error of about 5%.

Another error source for the heat flux estimate stems from the assumption that the thermal conductivity only depends on temperature. Besides temperature it also depends on pressure, quartz content, porosity, and fluid content of the rocks and may display rather large variability (Clauser & Huenges, 1995), although this variability generally decreases with depth. The uncertainty on the conductivity is about 15% (Clauser & Huenges, 1995).

The crustal heat production, which can have large lateral and vertical variation, constitutes a significant factor of uncertainty. For a given rock type the standard deviation of the measured heat production is very large; 40–60% of the mean value is not unusual (Kukkonen & Lahtinen, 2001; Abbady *et al.*, 2006; Brady *et al.*, 2006). Using this as indicative of the level of uncertainty on the assumed heat production it is clear that this is the largest error source of the heat flux estimate.

To summarize, uncertainties of the crustal field model and the crustal heat production are major sources of error, remanent magnetization, magnetic susceptibility and thermal conductivity are intermediate, whereas thermal boundary values and the 3SMAC model

constitutes minor sources of error on our heat flux estimate. Adding the error sources, which are independent, we find that the level of uncertainty of the magnetic crustal thickness estimate is about 34%, and the level of uncertainty of the heat flux estimate, including an error of 40–60% on the heat production, is 55–70%. Future work to refine these variables should reduce these errors and the current work should be seen as a first attempt to model crustal thickness and heat flux on a large scale in an area where constraining data is difficult to obtain.

6. Concluding remarks

The advent of increasingly complex and detailed magnetic field models encourages geophysical interpretation of the crustal field. We have derived a method to determine the magnetic crustal thickness and from this, to estimate the heat flux from a given crustal field model. Several studies have previously reported a connection between magnetic observations, Curie depth and heat flux, and such a method would be valuable in estimating heat flux underneath large ice sheets; a quantity which is otherwise difficult to obtain.

Using satellite magnetic data to determine the magnetic crustal thickness makes sence. Using magnetic field models as an intermediate stage rather than direct magnetic observations is natural as this allows for a separation of the field from various sources. We find that the equivalent source magnetic dipole (ESDM) method yields a reasonable estimate of the magnetic crustal thickness. Nevertheless there are some obvious deficiencies when estimating the magnetic crustal thickness from a field model. The fairly large level of crustal field model uncertainty poses a limitation on this study. There is hope that this will improve in future as better and more detailed field models are developed, especially as more accurate data are expected to become available with the Swarm satellite mission to be launched in 2010. An additional limitation is the lack of knowledge of the amount and distribution of remanent magnetization in the continental crust, and problems related to the fact that it is not possible to distinguish between variations of magnetic crustal thickness and magnetic susceptibility. This inevitably leads to ambiguity in the interpretation of the results. It appears to us that this difficulty can only be handled by incorporating a different type of data, for example lithological information, which could provide insight into the susceptibility variations. Despite these difficulties magnetic crustal field models can be used to obtain a reasonable estimate of the magnetic crustal thickness.

Estimating the heat flux from the magnetic crustal thickness is, however, a bigger challenge. It requires some important assumptions regarding the thermal state of the crust. The problem of modelling the crustal heat production dominates the uncertainty in the estimates. The large variability of heat production on a short length scale, even for a given type of rock, makes it very difficult to handle properly. Additional data such as lithologic information can, also in this case, significantly improve models of the geographical variation of heat production. Using a magnetic field model but no additional (e.g. lithologic) data as a basis for the heat flux estimate, as done here, has some difficulties, which is reflected in the high level of uncertainty. Even with improved field models, better knowledge of the remanent magnetization and the long wavelength variation of the magnetic crustal thickness there will still be uncertainty in the estimates of heat flux derived from magnetic data alone, due to the unknown heat production. Although reasonable estimates of the heat flux variation on a regional length scale can be derived using our approach, one should not expect that detailed information, including local variations of the heat flux, can be resolved. However, magnetic data contain information about the thermal conditions of the crust and it is very likely that

by combining magnetic information with for example seismic and lithological data much better heat flux estimates can be made than by using only one of the data sets.

References

Abbady, A.G.E., El-Arabi, A.M. & Abbady, A., 2006. Heat production rate from radioactive elements in igneous and metamorphic rocks in Eastern Desert, Egypt, *Applied Radiation and Isotopes*, **64**, 131-137, doi:10.1016/j.apradiso.2005.05.054.

Artemieva, I.M., 2006. Global 1°×1° thermal model TC1 for the continental lithosphere: Implications for lithosphere secular evolution, *Tectonophysics*, **416**, 245-277, doi:10.1016/j.tecto.2005.11.022.

Artemieva, I.M. & Mooney, W.D., 2001. Thermal thickness and evolution of Precambrian lithosphere: A global study, *J. Geophys. Res.*, **106**, 16.387-16.414.

Bassin, C., Laske, G. & Masters, G., 2000. The current limits of resolution for surface wave tomography in North America, *EOS Trans AGU*, **81**, F897.

Blakely, R.J., Brocher, T.M. & Wells, R.E., 2005. Subduction-zone magnetic anomalies and implications for hydrated forearc mantle, *Geology*, **33**, 445-448.

Brady, R.J., Ducea, M.N., Kidder, S.B. & Saleeby, J.B., 2006. The distribution of radiogenic heat production as a function of depth in the Sierra Nevada Batholith, California, *Lithos*, **86**, 229-244, doi:10.1016/j.lithos.2005.06.003.

Buchardt, S.L. & Dahl-Jensen, D., 2006. Estimating the basal melt rate at NorthGRIP using a Monte Carlo technique, *Ann. Glaciol.*, in press.

Christensen, N.I. & Mooney, W.D., 1995. Seismic velocity structure and composition of the continental crust: A global view, *J. Geophys. Res.*, **100**, 9761-9788.

Clark, D. A. & Emerson, D.W., 1991. Notes on rock magnetization characteristics in applied geophysical studies, *Exploration Geophysics*, **22**, 547-555.

Clauser, C. & Huenges, E., 1995. Thermal conductivity of rocks and minerals, *in Rocks Physics and Phase Relations: A Handbook of Physical Constants*, pp. 105-137, AGU Reference Shelf 3.

Clitheroe, G., Gudmundsson, O. & Kennett, B.L.N., 2000. The crustal thickness of Australia, *J. Geophys. Res.*, **105**, 13,697-13,713.

Collins, C.D.N., 1991. The nature of the crust-mantle boundary under Australia from seismic evidence, *in The Australian Lithosphere*, pp. 67-80, edt. Drummond, B.J., volume 17 Spec. Publ., Geol. Soc. of Aust..

Covington, J., 1993. Improvement of equivalent source inversion technique with a more symmetric dipole distribution model, *Phys. Earth Planet. Inter.*, **76**, 199-208.

Cull, J.P., 1991. Heat flow and regional geophysics in Australia, *in Terrestrial Heat Flow and Lithospheric Structure*, pp. 486-500, eds Cermak, V., & Rybach, L., Springer-Verlag, Berlin.

Dahl-Jensen, D., Mosegaard, K., Gundestrup, N., Clow, G.D., Johnsen, S.J., Hansen, A.W. & Balling, N., 1998. Past temperatures directly from the Greenland ice sheet, *Science*, **282**, 268-271.

Dahl-Jensen, D., Gundestrup, N., Gogineni, P. & Miller, H., 2003a. Basal melt at NorthGRIP modeled from borehole, ice-core and radio-echo sounder observations, *Ann. Glaciol.*, **37**, 207-212.

Dahl-Jensen, T., Larsen, T.B., Woelbern, I., Bach, T., Hanka, W., Kind, R., Gregersen, S., Mosegaard, K., Voss, P. & Gudmundsson, O., 2003b. Depth to Moho in Greenland: Receiver-function analysis suggests two Proterozoic blocks in Greenland, *Earth Planet. Sci. Lett.*, **205**, 379-393.

Durham, W.B., Mirkovich, V.V. & Heard, H.C., 1987. Thermal diffusivity of igneous rocks at elevated pressure and temperature, *J. Geophys. Res.*, **92**, 11,615-11,643.

Dyment, J. & Arkani-Hamed, J., 1998a. Equivalent source magnetic dipoles revisited, *Geophys. Res. Lett.*, **25**, 2003-2006.

Dyment, J. & Arkani-Hamed, J., 1998b. Contribution of lithospheric remanent magnetization to satellite magnetic anomalies over the world's oceans, *J. Geophys. Res.*, **103**, 15,423-15,441.

Fahnestock, M., Abdalati, W., Joughin, I., Brozena, J. & Gogineni, P., 2001. High geothermal heat flow, basal melt, and the origin of rapid ice flow in central Greenland, *Science*, **294**, 2338-2342.

Fox Maule, C., Purucker, M.E., Olsen, N. & Mosegaard, K., 2005. Heat flux in Antarctica revealed from satellite magnetic data, *Science*, **309**, 464-467, doi: 10.1126/science.1106888.

Frost, B.R. & Shive, P.N., 1986. Magnetic mineralogy of the lower continental crust, *J. Geophys. Res.*, **91**, 6513-6521.

Goes, S., Simons, F.J. & Yoshizawa, K., 2005. Seismic contraints on the temperature of the Australian uppermost mantle, *Earth Planet. Sci. Lett.*, **236**, 227-237.

Gregersen, S., Clausen, C. & Dahl-Jensen, T., 1988. Crust and upper mantle structure in Greenland, Recent Seismological Investigations in Europe, Proceedings of the 19th General Assembly of the ESC, Nauka, Moscow, 467-469.

Greve, R., 2005. Relation of measured basal temperatures and the spatial distribution of the geothermal heat flux for the Greenland ice sheet, *Ann. Glaciol.*, **42**, 424-433.

Grinsted, A. & Dahl-Jensen, D., 2002. A Monte Carlo-tuned model of the flow in the NorthGRIP area, *Ann. Glaciol.*, **35**, 527-530.

Gundestrup, N.S. & Hansen, B.L., 1984. Bore-hole survey at Dye 3, South Greenland, *J. Glaciol.*, **30**, 282-288.

Gundestrup, N.S., Dahl-Jensen, D., Hansen, B.L. & Kelty, J., 1993. Bore-hole survey at Camp Century, 1989, *Cold Reg. Sci. Technol.*, **21**, 187-193.

Hamoudi, M., Cohen, Y. & Achache, J., 1998. Can the thermal thickness of the continental lithosphere be estimated from Magsat data?, *Tectonophysics*, **284**, 19-29.

Hayling, K.L., 1991. Magnetic anomalies at satellite altitude over continent-ocean boundaries, *Tectonophysics*, **192**, 129-143.

Hemant, K. & Maus, S., 2005. Geological modeling of the new CHAMP magnetic anomaly maps using a geographical information system technique, *J. Geophys. Res.*, **110**, doi: 10.1029/2005JB003837.

Holme, R. & Olsen, N., 2002. Modelling of the geomagnetic field moves into a new era, *European Geologist*, **13**, 39-42.

Huybrechts, 1991. *The Antarctic ice sheet and environmental change: A three-dimensional modelling study*, PhD Thesis, Free University of Brussels.

Jaupart, C. & Mareschal, J.C., 1999. The thermal structure and thickness of continental roots, *Lithos*, **48**, 93-114.

Ketcham, R.A., 1996. Distribution of heat-producing elements in the upper and middle crust of southern and west central Arizona: Evidence from the core complexes, *J. Geophys. Res.*, **101**, 13,611-13,632.

Kinck, J.J., Husebye, E.S. & Larsson, F.R., 1993. The Moho depth distribution in Fennoscandia and the regional tectonic evolution from Archean to Permian times, *Precambrian Res.*, **64**, 23-51.

Kremenetsky, A.A., Milanovsky, S.Y.U. & Ovchinnikov, L.N., 1989. A heat generation model for continental crust based on deep drilling in the Baltic Shield, *Tectonophysics*, **159**, 231-246.

Kukkonen, I.T. & Lahtinen, R., 2001. Variation of radiogenic heat production rate in 2.8-1.8 Ga old rocks in the central Fennoscandian shield, *Phys. Earth Planet. Inter.*, **126**, 279-294.

Kukkonen, I.T., Jokinen, J. & Seipold, U., 1999. Temperature and pressure dependencies of thermal transport properties of rocks: implications for uncertainties in thermal lithosphere models and new laboratory measurements of high-grade rocks in the central Fennoscandian shield, *Surv. Geophys.*, **20**, 33-59.

Kuusisto, M., Kukkonen, I.T., Heikkinen, P. & Pesonen, L.J., 2006. Lithological interpretation of crustal composition in the Fennoscandian Shield with seismic velocity data, *Tectonophysics*, **420**, 283-299.

Langel, R.A. & Hinze, W.J., 1998. *The Magnetic Field of the Earth's Lithosphere; the Satellite Perspective*, Cambridge University Press, Cambridge.

Laske, G. & Masters, G., 1997. A global digital map of sediment thickness, *EOS Trans. AGU*, **78**, F483.

Lowes, F.J. & Olsen, N., 2004. A more realistic estimate of the variances and systematic errors in spherical harmonic geomagnetic field models, *Geophys. J. Int.*, **157**, 1027-1044.

Mandler, H.A.F. & Jokat, W., 1998. The crustal structure of central east Greenland: Results from combined land-sea seismic refraction experiments, *Geophys. J. Int.*, **135**, 63-76.

Mareschal, J.C. & Jaupart, C., 2004. Variations of surface heat flow and lithospheric thermal structure beneath the North American craton, *Earth Planet. Sci. Lett.*, **223**, 65-77, doi:10.1016/j.epsl.2004.04.002.

Maus, S., Rother, M., Hemant, K., Stolle, C., Luehr, H., Kuvshinov, A. & Olsen, N., 2006. Earth's lithospheric magnetic field determined to spherical harmonic degree 90 from CHAMP satellite measurements, *Geophys. J. Int.*, **164**, 319-330, doi: 10.1111/j.1365-246X.2005.02833.x.

Maus, S., Luehr, H., Rother, M., Hemant, K., Balasis, G., Ritter, P. & Stolle, C., 2007. Fifth-generation lithospheric magnetic field model from CHAMP satellite measurements, *Geochem. Geophys. Geosyst.*, **8**, Q05013, doi:10.1029/2006GC001521.

Mayhew, M.A., 1982a. An equivalent layer magnetization model for the United States derived from satellite altitude magnetic anomalies, *J. Geophys. Res.*, **87**, 4837-4845.

Mayhew, M.A., 1982b. Application of satellite magnetic anomaly data to Curie isotherm mapping, *J. Geophys. Res.*, **87**, 4846-4854.

Mayhew, M.A., 1985. Curie isotherm surfaces inferred from high-altitude magnetic anomaly data, *J. Geophys. Res.*, **90**, 2647-2654.

Mayhew, M.A., Wasilewski, P.J. & Johnson, B.D., 1991. Crustal magnetization and temperature at depth beneath the Yilgarn Block, Western Australia inferred from Magsat data, *Earth Planet. Sci. Lett.*, **107**, 515-522.

Nataf, H.-C. & Ricard, Y., 1996. 3SMAC: An a priori tomographic model of the upper mantle based on geophysical modeling, *Phys. Earth Planet. Inter.*, **95**, 101-122.

Neumann, N., Sandiford, M. & Foden, J., 2000. Regional geochemistry and continental heat flow: implications for the origin of the South Australian heat flow anomaly, *Earth Planet. Sci. Lett.*, **183**, 107-120.

North Greenland Ice Core Project members, 2004. High-resolution record of Northern Hemisphere climate extending into the last interglacial period, *Nature*, **431**, 147-151.

Okubo, Y., Graf, R.J., Hansen, R.O., Ogawa, K. & Tsu, H., 1985. Curie point depths of the island of Kyushu and surrounding areas, Japan, *Geophysics*, **53**, 481-494.

Olsen, N., 2002. A model of the geomagnetic field and its secular variation for epoch 2000 estimated from Ørsted data, *Geophys. J. Int.*, **149**, 454-462.

Olsen, N., Holme, R., Hulot, G., Sabaka, T., Neubert, T., Tøffner-Clausen, L., Primdahl, F., Jørgensen, J., Leger, J.-M., Barraclough, D., Bloxham, J., Cain, J., Constable, C., Golovkov, V., Jackson, J., Kotz, P., Langlais, B., Macmillan, S., Mandea, M., Merayo, J., Newitt, L., Purucker, M., Risbo, T., Stampe, M., Thomson, A. & Voorhies, C., 2000. Ørsted Initial Field Model, *Geophys. Res. Lett.*, **27**, 3607-3610.

Olsen, N., Luehr, H., Sabaka, T., Mandea, M., Rother, M., Tøffner-Clausen, L. & Choi, S., 2006. CHAOS - A model of Earth's magnetic field derived from CHAMP, Ørsted, and SAC-C magnetic satellite data, *Geophys. J. Int.*, **166**, 67-75.

Pollack, H.N., Hurter, S.J. & Johnson, J.R., 1993. Heat flow from the Earth's interior: Analysis of the global data set, *Rev. Geophys.*, **31**, 267-280.

Purucker, M.E. & Dyment, J., 2000. Satellite magnetic anomalies related to seafloor spreading in the South Atlantic ocean, *Geophys. Res. Lett.*, **27**, 2765-2768.

Purucker, M.E., Sabaka, T.J. & Langel, R.A., 1996. Conjugate gradient analysis: A new tool for studying satellite magnetic data sets, *Geophys. Res. Lett.*, **23**, 507-510.

Purucker, M.E., Langel, R.A., Rajaram, M. & Raymond, C., 1998. Global magnetization models with a priori information, *J. Geophys. Res.*, **103**, 2563-2584.

Purucker, M., Langlais, B., Olsen, N., Hulot, G. & Mandea, M., 2002. The southern edge of Cratonic North America: Evidence from new satellite magnetometer observations, *Geophys. Res. Lett.*, **29**, doi: 10.1029/2001GL013645, Art. No. 1342.

Ravat, D., Wang, B., Wildermuth, E. & Taylor, P.T., 2002. Gradients in the interpretation of satellite-altitude magnetic data: an example from central Africa, *J. Geodyn.*, **33**, 131-142.

Sabaka, T.J., Olsen, N. & Purucker, M.E., 2004. Extending comprehensive models of the Earth's magnetic field with Ørsted and CHAMP data, *Geophys. J. Int.*, **159**, 521-547.

Sandiford, M. & McLaren, S., 2002. Tectonic feedback and the ordering of heat producing elements within the continental lithosphere, *Earth Planet. Sci. Lett.*, **204**, 133-150.

Sass, J.H., Nielsen, B.L., Wollenberg, H.A. & Munroe, R.J., 1972. Heat flow and surface radioactivity at two sites in South Greenland, *J. Geophys. Res.*, **77**, 6435-6444.

Schlinger, C. M., 1985. Magnetization of lower crust and interpretation of regional magnetic anomalies: Example from Lofoten and Vesterålen, Norway, *J. Geophys. Res.*, **90**, 11,484-11,504.

Senthil Kumar, P. & Reddy, G.K., 2004. Radioelements and heat production of an exposed Archean crustal cross-section, Dharwar craton, south India, *Earth Planet. Sci. Lett.*, **224**, 309-324, doi:10.1016/j.epsl.2004.05.032.

Shapiro, N.M. & Ritzwoller, M.H., 2004. Inferring surface heat flux distributions guided by a global seismic model: particular application to Antarctica, *Earth Planet. Sci. Lett.*, **223**, 213-224, doi:10.1016/j.epsl.2004.04.011.

Shibutani, T., Sambrigde, M. & Kennett, B.L.N., 1996. Generic algorithm inversion for receiver functions with application to crust and uppermost mantle structure beneath eastern Australia, *Geophys. Res. Lett.*, **23**, 1829-1832.

Stampolidis, A. & Tsokas, G. N., 2002. Curie point depths of Macedonia and Thrace, N. Greece, *Pure Appl. Geophys.*, **159**, 2659-2671.

Tanaka, A., Okubo, Y. & Matsubayashi, O., 1999. Curie point depth based on spectrum analysis of the magnetic anomaly data in east and southeast Asia, *Tectonophysics*, **306**, 461-470.

Toft, P.B. & Haggerty, S.B., 1988. Limiting depth of magnetization in cratonic lithosphere, *Geophys. Res. Lett.*, **15**, 530-533.

Toft, P.B., Taylor, P.T., Arkani-Hamed, J. & Haggerty S.E., 1992. Interpretation of satellite magnetic anomalies over the West African Craton, *Tectonophysics*, **212**, 21-32.

Tsokas, G. N., Hansen, R. O. & Fytikas, M., 1998. Curie point depth of the Island of Crete (Greece), *Pure Appl. Geophys.*, **152**, 747-757.

Wasilewski, P. J. & Mayhew, M. A., 1992. The Moho as a magnetic boundary revisited, *Geophys. Res. Lett.*, **19**, 2259-2262.

White, R. S., McKenzie, D. & O'Nions, R. K., 1992. Oceanic crustal thickness from seismic measurements and rare Earth element inversions, *J. Geophys. Res.*, **97**, 19,683-19,715.